Progress In Electromagnetics Research M, Vol. 67, 137–146, 2018

Design and Performance Comparison of Permanent Magnet Brushless Motors and Switched Reluctance Motors for Extended Temperature Applications

Sree Ranjini K S[1, *] and S. Murugan[2]

Abstract—In-Service Inspection (ISI) plays a critical role in ensuring the safety and security of nuclear power plant and personnel. The limited access and high ambient temperature conditions impel the need for remote inspection techniques using semi automated vehicle. The electrical actuators driving the ISI robotic vehicle must satisfy the requirements of high operating temperature, high torque density, compact size and low weight. Currently, permanent magnet brushless motors are used due to its compact size and high efficiency. However, due to risk of demagnetization at high temperature as well as due to depleting resources of rare earth material alternate topologies without using permanent magnets shall be considered. This paper investigates the performance of Permanent Magnet (PM) brushless motor and Switched Reluctance (SR) motors for high temperature applications. SR motor is designed as per fundamental design equations satisfying the application requirements. Electromagnetic performance is verified by Finite Element Analysis (FEA) and thermal performance is verified by lumped parameter thermal analysis. Finally the performance of SR motor is compared with PM motor in terms of torque, efficiency, weight, cost and temperature rise.

1. INTRODUCTION

With applications in mining, aerospace and nuclear industries, demand for high temperature motors has increased in recent years [1]. Special care must be incorporated in design as well as material selection for development of such machines. In Service Inspection (ISI) of Fast Breeder Reactor (FBR) using semi-automated vehicle is such an application characterized by an operating temperature of 150°C [2]. High operating temperatures and high levels of radiation makes manual inspection of the plant infeasible. Any inspection under these circumstances can only be carried out by customized remote inspection techniques coupled with semi-automated vehicles. A compact, high temperature traction motor is required to drive the vehicle in the limited space. Due to the inherent advantages of high torque density, high efficiency and compact size, Permanent Magnet (PM) brushless machines are suitable for such kind of applications [3]. However, they employ rare earth permanent magnets for field excitation. With increase in ambient temperature, permanent magnets are subjected to greater risk of demagnetization [4]. Moreover, high temperature grades of these magnets are very expensive and subjected to uncertainty in market availability [1]. Hence possibilities of using alternate machine configurations without permanent magnets for extended temperature applications need to be explored.

Switched Reluctance (SR) motor, which works on reluctance principle for torque generation can be considered as an alternative candidate for brushless permanent magnet motors. Absence of permanent magnets, robust structure and phase independent operation makes SR motor competitive to PM

Received 25 February 2018, Accepted 28 March 2018, Scheduled 12 April 2018

* Corresponding author: Sree Ranjini K S (srks@igcar.gov.in).

[1] Homi Bhabha National Institute, Indira Gandhi Centre for Atomic Research, Kalpakkam, India. [2] Robotics, Irradiation-experiments and Mechanical Maintenance Division, Fast Reactor Technology Group, Indira Gandhi Centre for Atomic Research, Kalpakkam, India.

brushless motor. The design of SR motor having torque, power, speed range and efficiency values competitive to those of PM motor has been investigated for hybrid electric vehicles in [5]. Comparison studies for SR and PM motors have also been carried for electric bicycles [6] and electric brakes [7]. However, the plausibility of replacing PM motor with SR motor for high temperature, space saving high torque density application is not reported and demands a thorough investigation of electromagnetic and thermal performances. This paper presents a performance comparison between SR motor and PM brushless motor considering the application specifications of ISI semi-automated vehicle. Preliminary design is carried out based on general rules of thumb and guidelines for design of high performance practical configurations [8]. This design is then verified by Finite element analysis (FEA) which is considered to be an effective tool for virtual prototyping of machine. Electromagnetic and thermal models are linked due to temperature dependent properties of materials including copper, lamination steel, magnets and coolant. Hence, a coupled electromagnetic thermal analysis of motor is carried out to estimate the temperature rise in different parts of motor caused by electromagnetic losses. For simplicity and fast generation of results, thermal analysis is carried out using lumped parameter thermal model which is thermal counterpart of electric circuit analysis. A design of extended temperature, 12/8 inner rotor surface mounted permanent magnet motor is considered as the benchmark. The performance of each motor configuration is compared in terms of output torque, losses, efficiency, weight, material cost and average temperature. In this paper application requirements and specification of benchmark PM motor is described in Section 2. Section 3 describes the design process of SR motor and analysis using standard Finite Element Analysis (FEA) package. It also decribes the thermal modelling based on losses. A forced cooling system with nitrogen is proposed to increase lifetime of motors and to prevent the insulation breakdown. Section 4 describes the performance comparison of designed SR motor with benchmark PM motor. Final conclusions are drawn in Section 5.

2. APPLICATION SPECIFICATIONS

Table 1 shows the technical specifications of traction motor for semi automated vehicle which is finalized on the basis of simulation studies of the vehicle [2]. A typical four wheeled robotic vehicle equipped with non-destructive testing modules, capable of operating at ambient temperature of 150°C is considered for this application. The torque requirements for drive motor are derived by applying principles of vehicle dynamics. A motor torque of 2 Nm at a rated speed of 3500 rpm is necessary for operation of the vehicle. The acceleration and total weight of the motor is assumed to be $2\,m/s^2$ and 70 kg respectively. Based on the space allocation in the vehicle, volume of the motor is fixed as 150 mm × 150 mm × 150 mm. Totally enclosed non-ventilated cooling method is adopted and maximum current density is set to $5\,A/mm^2$.

The design of a surface mounted permanent magnet brushless motor compatible for high operating temperature is explained in [9]. Major issues in the design and operation of permanent magnet brushless motor at high temperatures are saturation of lamination steel, demagnetization of permanent magnets and increase in winding resistance. All these factors adversely affect machine's maximum torque capacity

Table 1. Application specifications for traction motor of ISI vehicle.

Parameter	Value
DC bus voltage	310 V
Rated Torque	2 Nm
Rated Speed	3500 rpm
Maximum Outer Diameter	120 mm
Maximum Length	90 mm
Ambient Temperature	150°C
Efficiency at ambient temperature	$> 75\%$
Weight	Minimum
Cooling	Nitrogen

and efficiency. These issues can be tackled if temperature within the motor is effectively managed by using high temperature materials, by a properly designed cooling system or combination of both. Iron cobalt vanadium (FeCoV) alloys offer high saturation density and lower core losses and is considered to be best material for compact design of motor working at high temperatures. Samarium cobalt magnets have good thermal endurance when compared to Neodymium Iron Boron magnets and can operate upto 350°C. For good thermal performance, inorganic insulation such as polyimide, amide-imide or ceramic can be used. Due to high bending radius, ceramic windings are not used [3]. Polyimide insulation that can withstand temperatures of 240°C is considered for winding insulation. Impregnation with high performance epoxy can further enhance the heat dissipation from windings. In FBR applications, where liquid sodium is used as coolant, water or air cannot be used in motor cooling system due to their reactive nature with sodium. In this context, Nitrogen is considered as the best candidate. SR and PM Motors are designed using the same materials for a fair comparison. The main objective behind the study is to explore the performance capabilities of SR motor for high temperature applications so that it can be considered as potential alternative to permanent magnet brushless motor.

3. DESIGN OF SWITCHED RELUCTANCE (SR) MOTOR

Switched Reluctance motor is a doubly salient motor which works on reluctance principle for torque generation. SR motor consists of laminated stator core with phase coils mounted around diametrically opposite poles. Rotor core is also laminated without permanent magnets or windings. Simple construction and high torque density makes it superior choice for different type of applications [10–12]. Torque is generated when the rotor poles tend to align with excited stator poles. The sequence of phase excitation to stator windings is determined by rotor position. The number of phases and combination of stator rotor poles defines the topology of SR motor [13]. The major disadvantage in the operation of SR motors is high torque ripple. This can be mitigated with increase in number of rotor poles [14]. Higher number of rotor poles leads to low torque ripple but at the cost of low saliency ratio and decreased torque output. Reduction in torque can be compensated by higher number of phases [15]. However, with higher number of phases, torque ripple is reduced, but increases complexity of motor structure as well as power. Considering all these factors, present study adopts design of inner rotor 4 phase, 8/6 SR motor. SR motor is designed to match the output torque of PM motor. The geometric dimensions of SR motors are derived as mentioned in [13] and [16]. The output torque is chosen as 2-Nm at a rated speed of 3500-rpm which is same as that of PM motor. The stator and rotor pole arc are set by the rules of Lawrenson's feasible triangle which determines the permissible combination [17]. The envelope dimensions of SR motor are calculated from torque equation.

$$T = kD_r L_{stk} \tag{1}$$

where k denotes the output coefficient, L_{stk} the stack length, and D_r the rotor diameter. The stator outer diameter D_s is estimated from the typical design ratio $\frac{D_r}{D_s}$ of 0.50–0.55 mentioned in [8, 13]. The airgap length, l_g, is roughly estimated as 0.5% of rotor diameter. Stator pole arc β_s and rotor pole arc β_r play a significant role in the performance of SR motor. In this study, $\beta_s = 21^\circ$ and $\beta_r = 23^\circ$ are selected.

Stator pole width t_s and rotor pole width t_r are calculated from Equations (2) and (3)

$$t_s = (D_r + 2l_g)\sin\frac{\beta_s}{2} \tag{2}$$

$$t_r = D_r \sin\frac{\beta_r}{2} \tag{3}$$

Stator yoke thickness y_s and rotor yoke thickness y_r must be sufficient to carry flux without saturation. They are calculated as 65% of respective pole width values. Rotor pole height, d_r, is taken about 50% of stator pole width. Stator pole height is calculated using formula

$$d_s = [D_s - D_r - 2(l_g + y_s)]/2 \tag{4}$$

Shaft diameter can be calculated from rotor diameter, rotor pole height and rotor yoke thickness. Slot fill factor is limited to 40% because of slot wall insulations and higher thickness of polyimide

insulated windings. Number of turns/poles is calculated as

$$Np = \frac{\Pi \mathrm{Vs}}{w_n t_s L_{stk} B_s m N_r} \tag{5}$$

where m represents the number of phases, V_s the DC supply voltage, w_n the speed in rad/sec, B_s the saturation flux density, and N_r the number of poles. The cross sectional views of benchmark PM motor and designed SR motor is shown in Fig. 1(a) and Fig. 1(b), respectively.

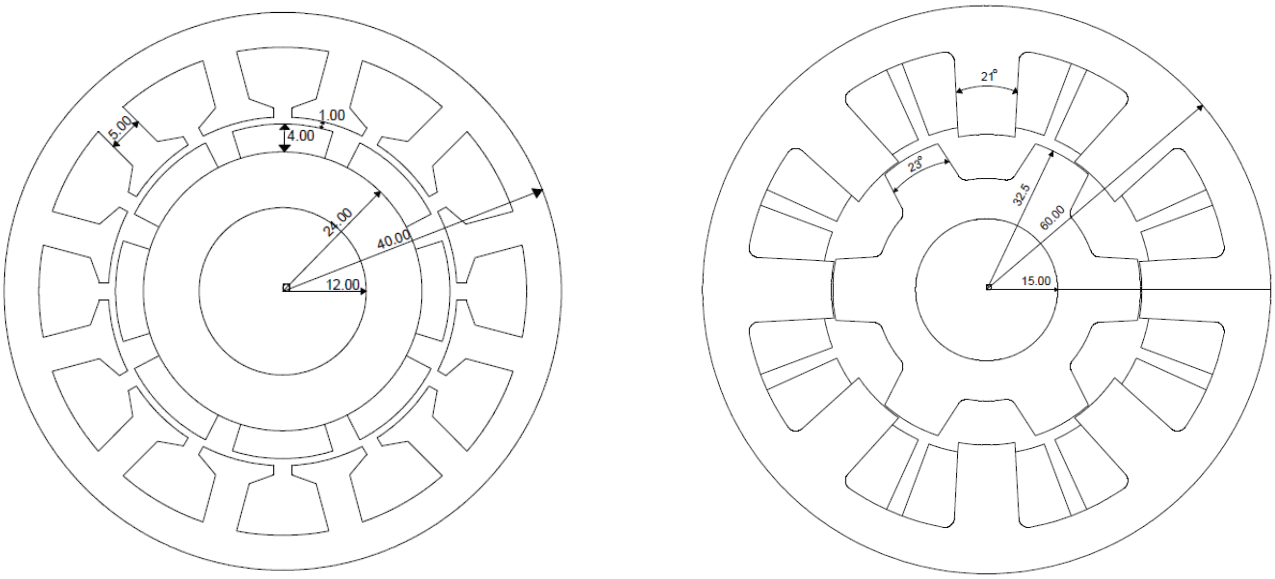

(a) (b)

Figure 1. Geometric overlay. (a) PM motor. (b) SR motor.

The stator and rotor dimensions of SR motor obtained by analytical design equations are verified by Finite Element Analysis (FEA). Taking account of geometric symmetry, only half of 2D geometry is constructed in standard FEA software package as shown in Fig. 2(a) and performance is verified with greater accuracy. Stator and rotor design are adjusted to achieve the target torque without serious magnetic saturation as per guidelines given in [18].

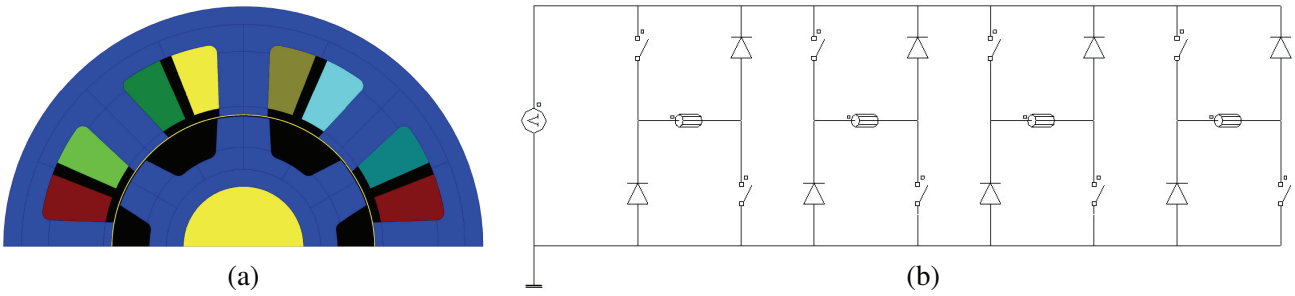

(a) (b)

Figure 2. Geometric crossection (a) half symmetrical 2D FEA model (b) four phase external drive circuit.

A four-phase asymmetrical half bridge converter with two switching devices and diodes per phase as shown in Fig. 2(b) is designed for driving SR motors. Field circuit coupled method solves magnetic vector potential and currents in the winding by combining finite element analysis of electromagnetic field with winding circuit equation through back-emf of stator windings. Turn off and turn on angles of

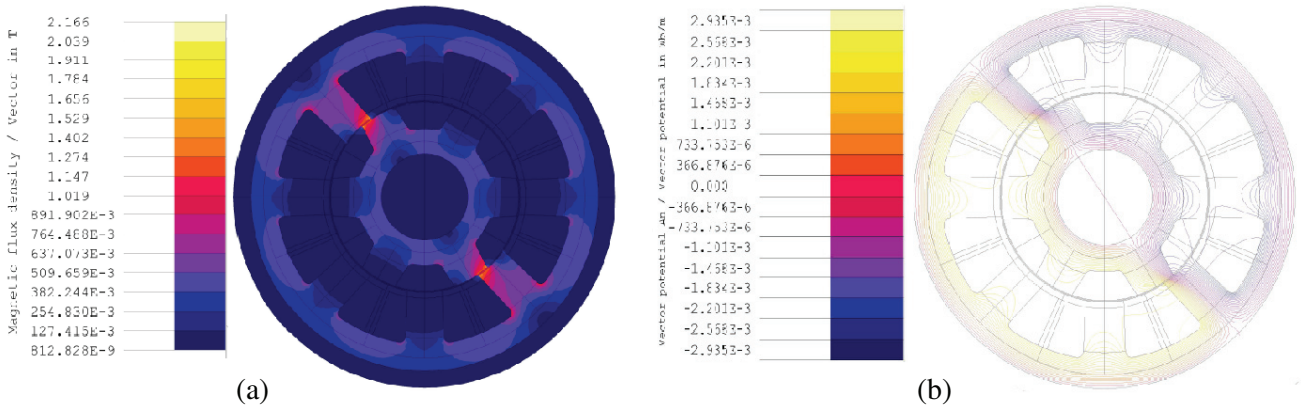

Figure 3. Magnetic field distribution of SR motor. (a) Magnetic flux density. (b) Magnetic flux path.

switches for driving the motor are computed from static torque curves for four phases. Optimum value of stator and rotor yoke is found by adjusting number of turns and preventing magnetic saturation. The current density for stator coil excitation was limited to $5\,\mathrm{A/mm^2}$ as recommended for natural cooled motors. The flux density distribution and flux path of SR motor is shown in Fig. 3(a) and Fig. 3(b) respectively. It is found that maximum flux density is less than the saturation flux density of iron cobalt vanadium alloy (2.25 T). Therefore, core material is being utilized fully by machine geometry.

After finalizing the dimensions, power losses which include copper loss and core loss are computed neglecting mechanical losses. In this paper, standard Jordan model of iron losses as shown in Equation (6) is used for analysis.

$$P_{Fe} = K_h f B_{pk}^2 + K_{ec} B_{pk}^2 f^2 + K_{ex} B_{pk}^{1.5} f^{1.5} \tag{6}$$

where K_h is the hysteresis coefficient, K_e the eddy current coefficient, K_{ex} the excess loss coefficient, B_{pk} the peak flux density, and f the frequency.

The copper power loss, P_{cu}, in SR motor is calculated as

$$P_{cu} = m I_{rms}^2 R_{r(T_{ref})} \left(1 + \alpha_r (T^{\circ}\mathrm{C} - T_{ref}^{\circ}\mathrm{C})\right) \tag{7}$$

where I_{rms} denotes the rms current, T the operating temperature, $R_{r(T_{ref})}$ the resistance at temperature T_{ref}, and α_r the linear coefficient of temperature dependence of resistance.

Due to high ambient temperature and number of phases, copper loss is prominent and contributes to major part of the total losses. Once the losses are estimated from electromagnetic model, values are exported to thermal model for finding temperature rise.

3.1. Thermal Model & Cooling Design

In this analysis, a lumped parameter thermal model of SR motor is established with MOTORCAD software to obtain very fast and accurate results of temperature rise within the machine [19]. Thermal circuit of different parts of motor have been combined to obtain a complete thermal model of motor. Heat transfer occurs by conduction within solid and laminated components, where as it occurs by convection within air or any other cooling fluids. For thermal modelling stator and rotor of SR motors are considered as hollow cylinders, whereas stator teeth and rotor teeth are considered as partial hollow cylinders. Axial shaft is modelled as long beam and heat transfer is taken along axial direction. Conductive heat transfer in a hollow cylinder containing heat sources can be solved using Fourier's law [20].

$$\frac{1}{r}\frac{\partial}{\partial r}\left[k_r \frac{\partial T}{\partial r}\right] + \frac{1}{r^2}\frac{\partial}{\partial \theta}\left[k_\theta \frac{\partial T}{\partial \theta}\right] + \frac{\partial}{\partial z}\left[k_z \frac{\partial T}{\partial z}\right] + q^{\circ} = \rho c_p \frac{\partial T}{\partial t} \tag{8}$$

where q represents the heat source represented by losses, (k_r, k_θ, k_z) the thermal conductivity in cylindrical co-ordinate system, ρ the density, c_p the specific heat capacity, and T the temperature.

There exist a number of conductive paths inside machine such as from winding copper to stator tooth and stator back iron, from stator back iron to stator bore. Conductive thermal resistance, R_{cond}, is calculated as

$$R_{cond} = L/KA \tag{9}$$

where L and A denote the length and path area from geometry, and K denotes the thermal conductivity of material.

External convection and radiation resistances are used for heat transfer from outside of machines to ambient. The convection heat transfer R_{conv} and radiation heat transfer R_{rad} equations are calculated by following formulas

$$R_{conv} = 1/(Hc \cdot A) \tag{10}$$

$$R_{rad} = 1/(Hr \cdot A) \tag{11}$$

where H_c and H_r denote specific convection and radiation heat transfer coefficients, respectively.

Convection coefficient, H_c, is usually made dimensionless and is derived from Equation (12)

$$N_u = \frac{H_c L}{K} = f(R_a, P_r) \tag{12}$$

in the cases of natural convection and forced convection, from Equation (13)

$$N_u = \frac{H_c L}{K} = f(R_e, P_r) \tag{13}$$

where L is the characteristic length, N_u the Nusselt number, R_e the Reynold's number, R_a the Rayleigh's number, and and P_r the Prandtl's number [20]. Thermal resistance values are automatically calculated from motor dimensions and material data. Thermal physical properties of used materials are tabulated in Table 2.

Table 2. Thermal physical properties of materials used in the analysis.

Materials	Density (Kg/m^3)	Specific heat capacity (J/KgK)	Conductivity (W/mK)
Iron Cobalt Vanadium alloy	8110	460	29.8
Copper	8933	385	401
Polyimide Insulation	1430	1130	0.35
Epoxy Impregnation	1200	1500	0.22
Air	1.225	1006.43	0.024
Nitrogen	1.041	1040	0.027

The knowledge of thermal resistances of motor components decides the accuracy of calculation. As the motor operates continuously in high ambient temperature environment, temperature increases due to losses. This can lead to damage of insulation material. To meet the temperature limits and to increase life time of motors, an appropriate cooling method is proposed. Considering inspection field environment of nuclear reactors, water cooling and any other type of liquid cooling methods is not advisable. Nitrogen is already provided at the inspection field to create an inert atmosphere. Taking this as an advantage, a cooling system with ducts on stator and rotor sides is proposed with nitrogen as coolant. Flow rate of nitrogen is fixed to 0.025 m^3/s, and temperature is fixed to 40°C. Heat transfer from external surface of motor occurs by convection and radiation. Two inlet and two outlet ducts are provided for coolant flow, and direction of coolant flow is shown in Fig. 4. The temperatures in different parts of motor with and without cooling are shown in Figs. 5(a) and 5(b), respectively.

It is observed that the proposed cooling method shows 63% decrease in rotor temperature compared to naturally cooled SR motor. Temperatures in housing,stator and winding on average are reduced by 37%, 34.3%, and 39%, respectively. With the proposed cooling system, the deterioration of insulation in windings can be effectively managed, and operating life time of motors can be increased. It also provides additional advantage of increased current density, thus delievering higher torque.

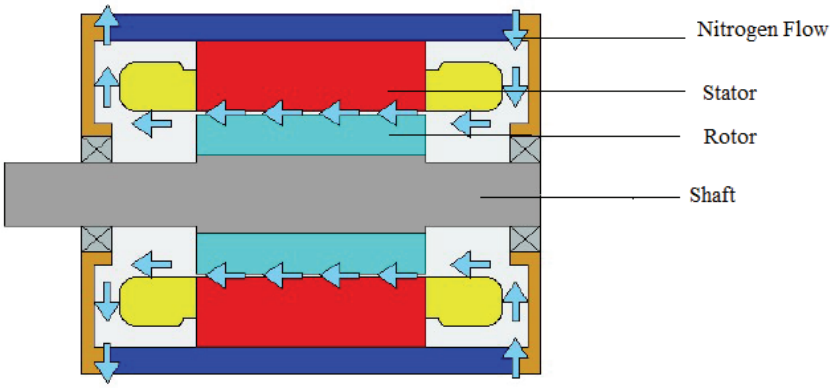

Figure 4. Proposed cooling system for SR motor.

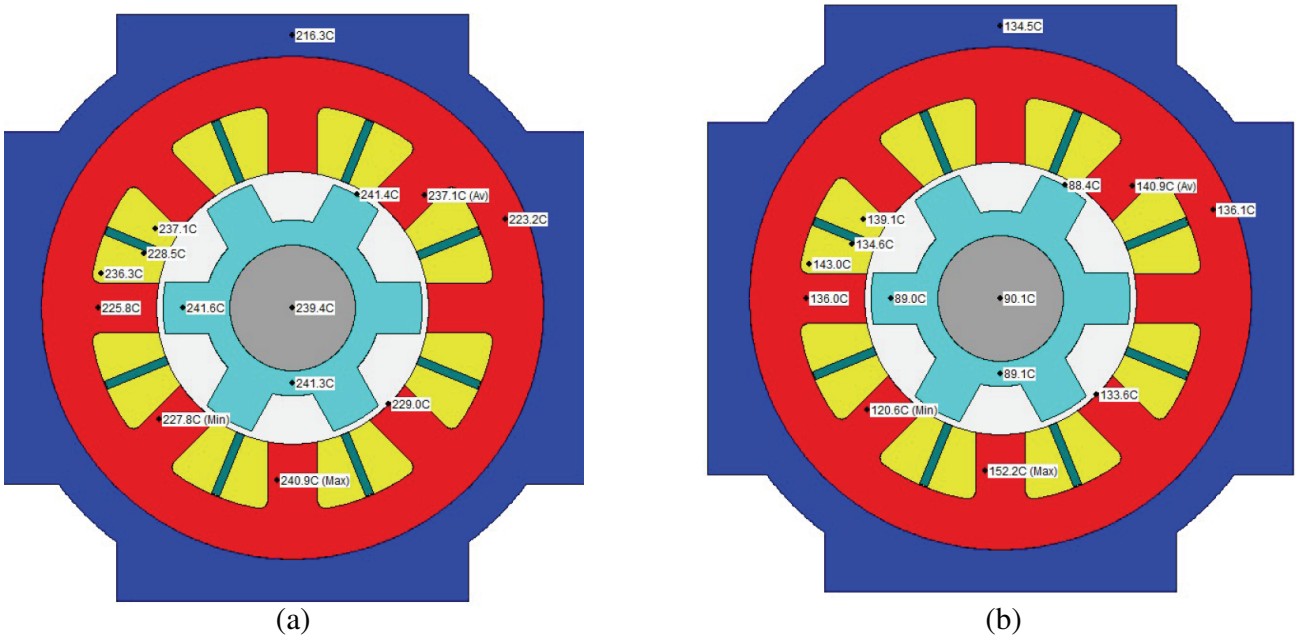

Figure 5. Temperature distribution of SR motor (a) without cooling (b) with cooling.

4. RESULTS AND DISCUSSIONS

The performance comparison of PM motors and SR motors is made in terms of torque, efficiency, weight, cost and temperature rise.

4.1. Torque

To meet the output torque requirements, the outer diameter and stack length of SR motor are increased to 120 mm and 88 mm respectively. SR motor requires greater dimensions than brushless permanent magnet motor for producing the required torque. This can ultimately increase the envelope size of traction motor in the inspection vehicle. The torque characteristics of SR motor and PM motor are shown in the Fig. 6(a). It is found that at rated speed of operation, the torque ripple is high for SR motor compared to brushless motor. This is due to inherent nonlinear property of inductance according to current and rotor position and due to the doubly salient structure of stator and rotor [15]. Torque

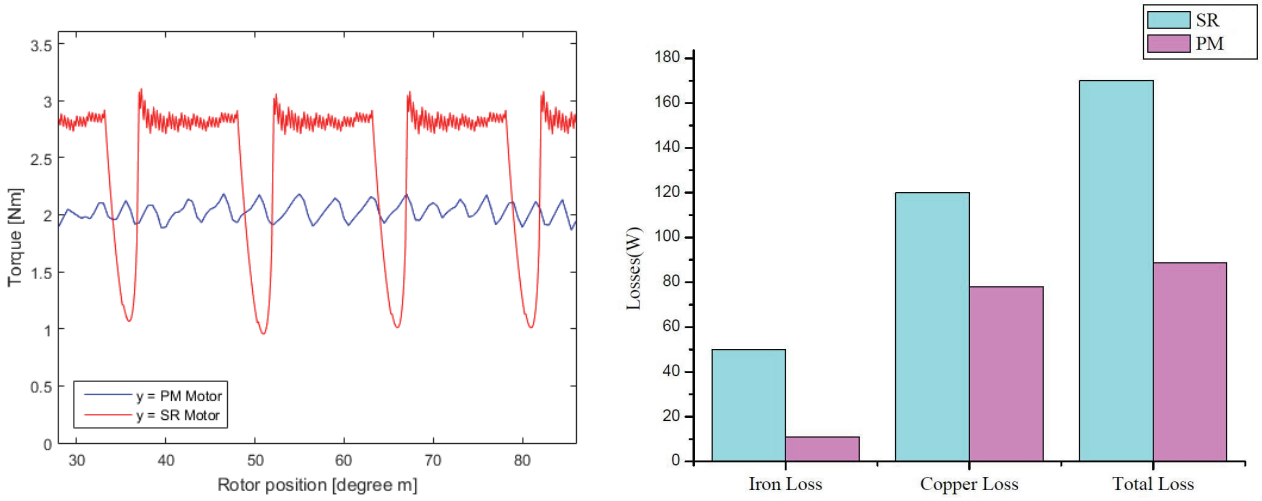

Figure 6. Performance comparison of SR and PM motors. (a) Torque. (b) Losses.

ripple can be further reduced by optimizing the design, manipulating stator rotor pole arc or by using advanced control techniques [21].

4.2. Efficiency

In permanent magnet motors, permanent magnets act as a source of excitation in addition to the stator windings. Hence torque generation is contributed partly by permanent magnets and partly by stator excitation current. SRM on other hand, require greater amount of stator windings to generate equivalent torque. Moreover, high ambient temperature also causes increase in resistance of windings which further add to copper loss. Copper loss contributes major part to the total losses thus reducing the efficiency of SR motor to about 73.5% at 150°C while that of permanent magnet motor is about 85.84%. Fig. 6(b) shows the comparison in terms of losses of SR and PM motor.

4.3. Weight and Cost

Weight of SR motor is on higher side than PM motor, due to its increased weight of iron and windings. Table 3(a) shows the weight of active parts of PM motor and SR motor (excluding weight of shaft and housing). The difference in weight is about 0.5 kg which is insignificant as compared with the weight of ISI vehicle, which is around 80 kg. Considering manufacturing and material cost as per the current market price [6], PM motors becomes expensive option due to the presence of high temperature permanent magnets. The per unit cost of high temperature permanent magnet is about 12–20 USD which is much higher than conventional ferrite or alnico magnets. Apart from this, polyimide coated copper conductors and high saturation iron cobalt vanadium alloy typically cost about 16.7–33.4 USD/kg and 30–100 USD/kg respectively. Considering the required specification, material price of SR motor costs about 250–300 USD where as that of PM motor costs about 350–400 USD.

4.4. Temperature Rise

Thermal performance of SR motor with natural and forced cooling is compared with that of permanent magnet motor with natural cooling in Table 3(b). It is found that thermal performance of SR motor with forced cooling is better than that of PM motors. The winding temperature of permanent magnet brushless motors is found to be 44.1°C greater than SR motor with forced cooling. However, without cooling, temperature in various parts of SR motor is found higher than that of permanent magnet motors. The provision of additional cooling system can also increase the cost of SR motor upto 30%.

Table 3. Performance comparison of SR and PM motors, (a) weight, (b) temperature.

Active parts	SRM	PM
Iron (kg)	2.5	1.9
Magnet (kg)	-	0.2
Copper (kg)	0.7	0.5
Total (kg)	3.2	2.7

(a)

Motor Part	SRM(°C)	PM(°C)
Winding	140	185.1
Housing	136	190
Rotor	89	182
Stator	136	181
Shaft	90	177
Bearing	125	174

(b)

5. CONCLUSION

This paper primarily discusses the feasibility of SR motors for application in traction of ISI vehicle operating at high ambient temperature of 150°C. Design of SR motor compatible for high temperature, and of same torque requirements of bench mark PM brushless motor is carried out and verified using Finite Element Analysis. A lumped parameter thermal analysis is carried out with MOTORCAD to predict the temperature rise in different parts of SR motor. A cooling system with nitrogen as coolant is proposed for safe and prolonged use of SR machine. With the proposed cooling method SR motor shows decrease of 34% in winding temperature. SR motors is compared with PM motor in terms of torque, efficiency, weight and temperature rise. The designed SR motor is attractive in terms of cost and simplicity but has disadvantages of high torque ripple and increased dimensions. SR motor is slightly heavier than PM motors; however, considering the application, difference in weight is insignificant. Efficiency of SR motor is less than PM motors due to increased copper losses. Temperature rise in different parts of SR motor with forced cooling is much less than PM motors, but thermal performance of SR motors without cooling is inferior to PM motors. PM motor is recommended for high efficiency, low weight and good thermal performance; bearing the risk of high cost and uncertainty in availability of magnets. SR motor is a potential candidate for this application if proper cooling is provided. Though SR motor is inferior to PM motor in terms of size, efficiency and torque ripples, it has key advantages such as no risk of demagnetization at high temperature, low cost and easy availability. The designer can make an appropriate trade-off between the above mentioned parameters to choose the best option for ISI application.

REFERENCES

1. Bar-Cohen, Y., *High Temperature Materials and Mechanisms*, ISBN 9781466566453, CRC Press, Mar. 2014.
2. Ashutosh, S. P., C. Rajagopalan, V. Rakesh, S. Rajendran, S. Venugopal, K. V. Kasiviswanathan, and T. Jayakumar, "Evolution in the design and development of the in-service inspection device for the indian 500 mwe fast breeder reactor," *Nucl. Eng. Des.*, Vol. 241, No. 9, 3719–3728, 2011.
3. Sakai, K., H. Karasawa, T. Yagisawa, H. Mitsui, Y. Sawada, S. Ohta, and M. Kai, "Development and characteristics of servomotor for use under high temperature and radiation flux conditions," *Electr. Eng. Jpn.*, Vol. 119, No. 4, 52–65, 1997.
4. Gieras, J. F., *Material Engineering*, 27–69, Springer, Dordrecht, Netherlands, 2008.
5. Kiyota, K. and A. Chiba, "Design of switched reluctance motor competitive to 60-kw ipmsm in third-generation hybrid electric vehicle," *IEEE Transactions on Industry Applications*, Vol. 48, No. 6, 2303–2309, 2012.
6. Kerdsup, B. and N. H. Fuengwarodsakul, "Performance and cost comparison of reluctance motors used for electric bicycles," *Electrical Engineering*, Vol. 99, 475–486, Jun. 2017.
7. Omekanda, A. M., B. Lequesne, H. Klode, S. Gopalakrishnan, and I. Husain, "Switched reluctance and permanent magnet brushless motors in highly dynamic situations: A comparison in the context of electric brakes," *Conference Record of the 2006 IEEE Industry Applications Conference Forty-First IAS Annual Meeting*, Vol. 3, 1570–1577, Oct. 2006.

8. Chang, L., "Design procedures of a switched reluctance motor for automobile applications," *Canadian Conference on Electrical and Computer Engineering*, Vol. 2, 947–950, IEEE, 1996.
9. Ranjini, K. S., R. Chellapandian, S. Murugan, and S. Venugopal, "Design and analysis of brushless servomotor for in-service inspection of PFBR," *2015 Annual IEEE India Conference (INDICON)*, 1–5, Dec. 2015.
10. Michon, M., S. D. Calverley, and K. Atallah, "Operating strategies of switched reluctance machines for exhaust gas energy recovery systems," *IEEE Trans. Ind. Appl.*, Vol. 48, 1478–1486, Sept. 2012.
11. Sundaram, M., P. Navaneethan, and T. D. Kumar, "Design and development of energy efficient submersible switched reluctance motor," *Journal of Engineering & Technology*, Vol. 4, No. 1, 2014.
12. Widmer, J. D., R. Martin, and M. Kimiabeigi, "Electric vehicle traction motors without rare earth magnets," *Sustainable Mater. Technol.*, Vol. 3, 7–13, 2015.
13. Shoujun, S., L. Weiguo, D. Peitsch, and U. Schaefer, "Detailed design of a high speed switched reluctance starter/generator for more/all electric aircraft," *Chin. J. Aeronaut.*, Vol. 23, No. 2, 216–226, 2010.
14. Bilgin, B., A. Emadi, and M. Krishnamurthy, "Design considerations for switched reluctance machines with a higher number of rotor poles," *IEEE Trans. Ind. Electron.*, Vol. 59, 3745–3756, Oct. 2012.
15. Anwar, M. N., I. Husain, and A. V. Radun, "A comprehensive design methodology for switched reluctance machines," *IEEE Trans. Ind. Appl.*, Vol. 37, 1684–1692, Nov. 2001.
16. Miller, T. J. E., *Switched Reluctance Motors and Their Control*, Magna Physics, 1993.
17. Lawrenson, P., J. Stephenson, P. Blenkinsop, J. Corda, and N. Fulton, "Variable-speed switched reluctance motors," *IEE Proceedings B (Electric Power Applications) IET,*, Vol. 127, 253–265, 1980.
18. Chiba, A., K. Kiyota, N. Hoshi, M. Takemoto, and S. Ogasawara, "Development of a rare-earth-free sr motor with high torque density for hybrid vehicles," *IEEE Trans. Energy Convers.*, Vol. 30, No. 1, 175–182, 2015.
19. Boglietti, A., A. Cavagnino, and D. Staton, "Thermal analysis of TEFC induction motors," *Conference Record of the 2003 IEEE Industry Applications Conference 38th IAS Annual Meeting*, Vol. 2, 849–856, 2003.
20. Rouhani, H., J. Faiz, and C. Lucas, "Lumped thermal model for switched reluctance motor applied to mechanical design optimization," *Mathematical and Computer Modelling*, Vol. 45, No. 5, 625–638, 2007.
21. Suryadevara, R. and B. Fernandes, "Control techniques for torque ripple minimization in switched reluctance motor: An overview," *2013 8th IEEE International Conference on Industrial and Information Systems (ICIIS)*, 24–29, 2013.